

# Crystallization of a Bi–Pb–Fe–Cd–O glass under magnetic annealing

YI HU

*Department of Materials Engineering, Tatung Institute of Technology, Taipei, Taiwan*

Magnetic annealing with a tunable solenoid magnetic field from 0–240 G, was conducted on a Bi–Pb–Fe–Cd–O glass containing 20% Fe<sub>2</sub>O<sub>3</sub>, which was prepared by the melt-quenching process. The crystalline phases of the annealed samples were identified as  $\gamma$ -Bi<sub>2</sub>O<sub>3</sub> and BiFeO<sub>3</sub>. Evidence of the formation of the crystalline BiFeO<sub>3</sub> which was strongly magnetically enhanced at the surface of the samples, was obtained from X-ray diffraction patterns and EPR spectra. Based on the structure transition of Fe<sup>3+</sup> ions, a crystallization mechanism for the BiFeO<sub>3</sub> crystals under magnetic annealing has been proposed.

## 1. Introduction

Glass-ceramics made by controlled crystallization of special glasses have become one of the new types of engineering materials developed during the past few decades. This kind of glass-ceramic exhibits high density with good mechanical properties. Its production process also provides a good means of combining a wide range of unusual properties of glasses and ceramics. Therefore, a controlled crystallization process of glass has been developed into an independent new field of technology and is now commonly employed in heat treatment [1], and additions of nucleation agents [2,3] have been successfully adapted for the crystallization process, producing many high-quality glass-ceramic materials. However, these techniques are limited by our understanding of the mechanisms of crystallization that are involved in the formation of crystal nuclei and their subsequent growth. It is therefore necessary to exploit a different process to obtain more information on the crystallization mechanisms. In this work, magnetic annealing was used to study the crystallization of a glass.

The application of a magnetic field during heat treatment is termed “magnetic annealing” and is frequently applied to many alloy systems [4–6]. Yet, in the literature, the effects of magnetic annealing on the crystallization of glasses has not been reported. When certain alloys are magnetically annealed, they may develop a permanent magnetic anisotropy. These induced anisotropies are of considerable interest to study the basic magnetic phenomena and to design magnetic materials for applications. However, materials for magnetic annealing should have high magnetic susceptibility [7–9]. In this study, we chose the iron-containing magnetic glass for the magnetic crystallization experiment. The aim of the present investigation was to examine the effect of magnetic annealing on the crystallization of a magnetic glass.

## 2. Experimental procedure

### 2.1. Preparation of glass samples

Bismuth oxide and lead oxide glasses have been studied for their good infrared transmission [10–12]. However, systems containing only bismuth oxide and lead oxides are difficult to make into glass. In order to produce glass from these oxides, some modifying oxides have been used to increase the glass-forming range. Additions of ferric and cadmium oxides, which act as glass-forming stabilizers, resulted in a large region of glass formation [12]. Therefore, the high solubility of Fe<sub>2</sub>O<sub>3</sub> in bismuth–lead glasses is suitable for the present study, to produce magnetic glasses.

A glass with the composition 40Bi<sub>2</sub>O<sub>3</sub>–25PbO–20Fe<sub>2</sub>O<sub>3</sub>–15CdO in molar ratio was prepared by the melting and quenching process. Reagent-grade bismuth carbonate (BiCO<sub>3</sub>, > 99%), lead oxide (PbO, > 99%), iron oxide (Fe<sub>2</sub>O<sub>3</sub>, > 99%), and cadmium oxide (CdO, > 99%) were completely mixed, preheated at 800 °C for 1 h, and then melted at 1200 °C for 30 min in air in alumina crucibles. Glass sheets were formed by pressing the melt between two copper plates. These glass sheets were subsequently annealed at 200 °C for 12 h to release the internal stress. The as-quenched glass sheets have a thickness of about 1.2 mm and were double-sided polished to about 0.5 mm thickness and cleaned with alcohol in an ultrasonic bath at room temperature.

### 2.2. DSC thermal analysis

A differential scanning calorimetry (DSC, Perkin–Elmer DSC-4) was used to study the crystallization process of glasses and to predetermine the heat-treatment temperature [13]. In the present study, DSC was conducted with heating rates from 5 °C min<sup>-1</sup> in air and a typical DSC curve of the glasses is shown in Fig. 1. An endothermic peak due to the glass transition ( $T_g \sim 610$  K) and an exothermic peak due to crystallization ( $T_c \sim 690$  K) are clearly observed.

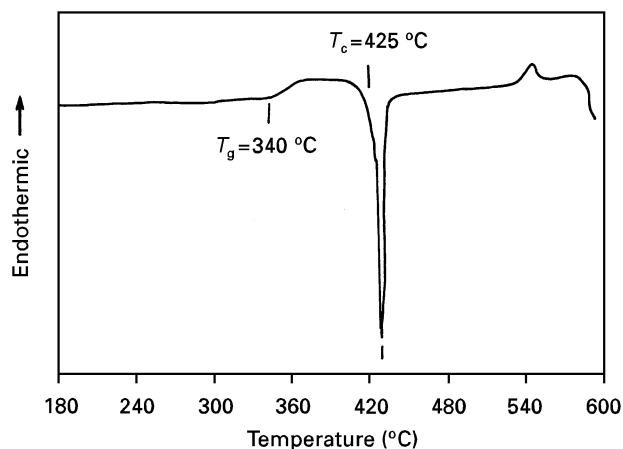
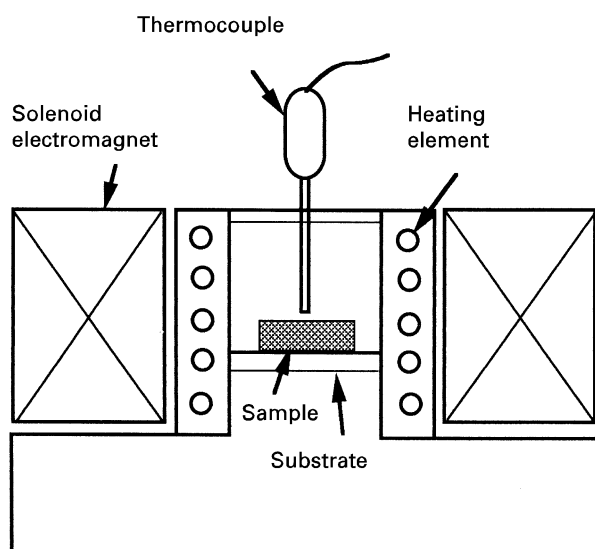
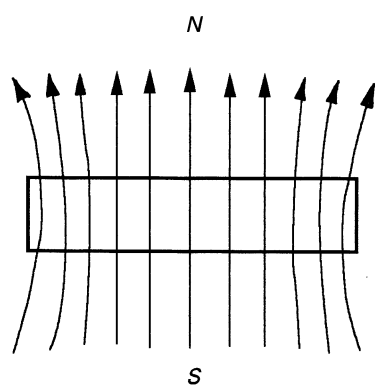


Figure 1 DSC curve for the melt-quenched glass sample. Heating rate =  $10^{\circ}\text{C min}^{-1}$ .  $T_g$  and  $T_c$  are the glass transition and crystallization temperatures, respectively.



(a)



(b)

Figure 2 (a) The illustration of the apparatus for the magnetic annealing. (b) Schematic plots of the magnetic field of the applied solenoid.

### 2.3. Magnetic annealing

A schematic illustration of the apparatus for magnetic annealing is shown in Fig. 2a and the magnetic field of the applied solenoid is sketched in Fig. 2b. The solenoid magnetic field is d.c. tunable from 0–240 G. The strength of the applied magnetic field on the samples

was adjusted experimentally [14]. The sample was put on an  $\text{Al}_2\text{O}_3$  substrate at the centre of the solenoid and was heated in air at a predetermined temperature, of  $520^{\circ}\text{C}$ , which is higher than  $T_c$ , for 30 min with a heating rate of  $5^{\circ}\text{C min}^{-1}$ .

### 2.4. Structure investigation

The crystalline phase of the samples (bulk and powder) was studied by X-ray diffraction (XRD) using  $\text{CuK}_\alpha$  radiation. The surfaces of the annealed samples were etched and investigated by a scanning electron microscopy (SEM). The etching solution was composed of 0.05 M HCl and 0.1 M acetic acid in alcohol and the etching process took 1 min. Electron paramagnetic resonance (EPR) spectroscopy was used to investigate the ionic state of iron.

### 3. Results and discussion

XRD patterns for glass and annealed glass-ceramic samples without an applied magnetic field are shown in Fig. 3. The sample quenched from the melt and annealed at  $200^{\circ}\text{C}$  shows an amorphous state with a halo at  $2\theta = 25^{\circ}$  as shown in Fig. 3a. XRD patterns of the powder and the bulk surface of the samples without an applied magnetic field are shown in Fig. 3b and c, respectively. Comparing the observed patterns with those known for lead, bismuth, cadmium, and iron oxides and compounds, the major crystalline phase was identified as  $\gamma\text{-Bi}_2\text{O}_3$  [15, 16] and the minor phase to be  $\text{BiFeO}_3$  [17]. Fig. 3d shows the X-ray bulk diffraction pattern of the sample after removing the sample's surface layer. The diffraction patterns of Fig. 3b and d are very similar, whereas that of Fig. 3c shows a higher intensity of  $\text{BiFeO}_3$  phase. This indicates that the volume of the  $\text{BiFeO}_3$  crystalline phase is slightly higher on the surface than in the interior of the annealed sample.

On studying the XRD patterns of samples with applied magnetic field, as shown in Fig. 4, the intensity of  $\text{BiFeO}_3$  crystalline phase in the bulk diffraction is seen to have become strong when the sample was annealed with a magnetic field (240 G) as shown in Fig. 4b. However, when the surface of the magnetically annealed sample was removed by grinding, the diffraction pattern (Fig. 4c) became similar to the powder diffraction pattern in Fig. 4a. The strongly induced peaks can be explained by the high volume fraction of  $\text{BiFeO}_3$  phase dispersed in the vicinity of the surface.

From the EPR spectrum, as shown in Fig. 5a, it can be found that the glassy samples are characterized by an intense resonance at  $g = 4.23$ , which is due to the tetrahedrally coordinated  $\text{Fe}^{3+}$  ions, as reported in the literature [18, 19]. This peak is characteristic of isolated ferric ions and usually occurs in non-ferromagnetic materials. In addition to the  $g = 4.23$  signal, a second resonance with low intensity is also exhibited at  $g = 2.20$  which is attributed to the presence of  $\text{Fe}^{3+}$  ions in octahedral sites [20]. Actually, the glass contains a mixed valence ( $2+$  and  $3+$ ) of ferric irons and the molar ratio of  $\text{Fe}^{2+}/(\text{Fe}^{2+} + \text{Fe}^{3+})$  is larger than 0.5 in most cases

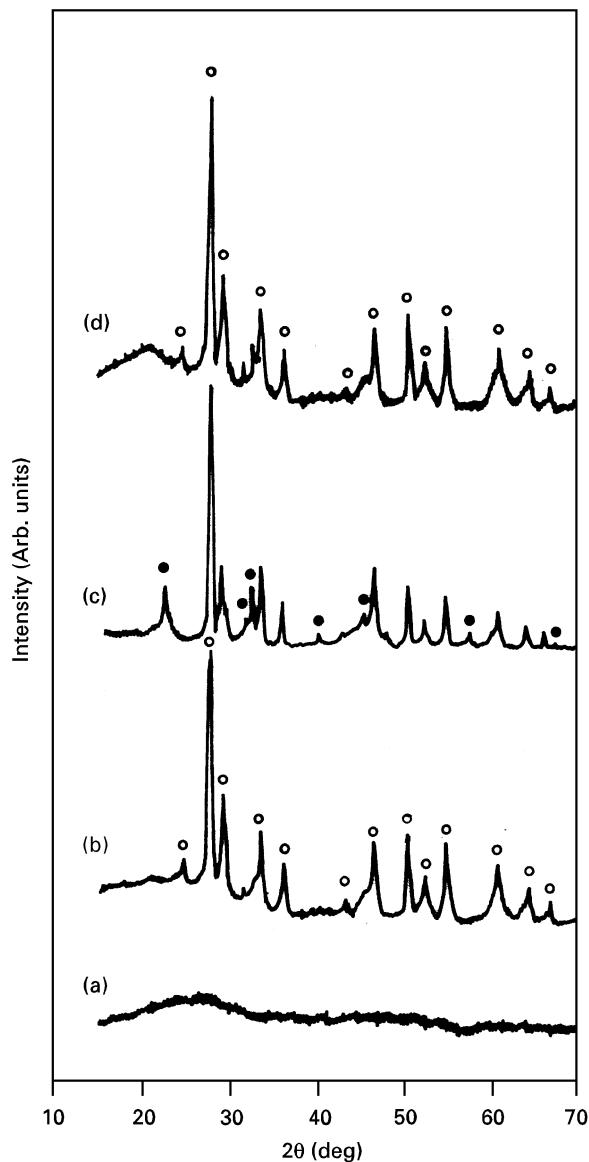


Figure 3 XRD patterns of (a) the original glass powder, (b) the ground powder of the annealed sample, (c) the bulk surface of the annealed sample, and (d) the inner layer of the annealed sample without applied field. (○)  $\gamma$ - $\text{Bi}_2\text{O}_3$ , (●)  $\text{BiFeO}_3$ .

[21–23]. The ferric iron  $\text{Fe}^{2+}$  acts as a network modifier and has octahedral coordination with oxygen. However, it can also be found that the ferric iron,  $\text{Fe}^{3+}$ , can be a glass network former if it is in tetrahedral coordination.

The intensities of the  $\text{Fe}^{3+}$  resonance peaks in Fig. 5 are listed in Table I. The fraction of the  $[\text{Fe}^{3+}]$  changing from  $[\text{Fe}^{3+}\text{O}_4]$  to  $[\text{Fe}^{3+}\text{O}_6]$  was obtained from the decrease of the intensity at  $g = 4.23$ . The degree of oxidation of  $[\text{Fe}^{2+}]$  was obtained from the increase in the overall intensity at  $g = 4.23$  and  $2.20$ . It was found that the intensity of the resonances around  $g = 2.20$  increased for both of the samples annealed without and with magnetic field. This indicates that the fraction of  $\text{Fe}^{3+}/\text{Fe}^{2+}$  increases during heat treatment. A more significant increase of the resonance at  $g = 2.20$  was observed in the sample with magnetic annealing. Evidence of the increase of  $\text{Fe}^{3+}$  in the vicinity of the surface could also be obtained by EPR analysis of the surface layer of sample in Fig. 5c. This

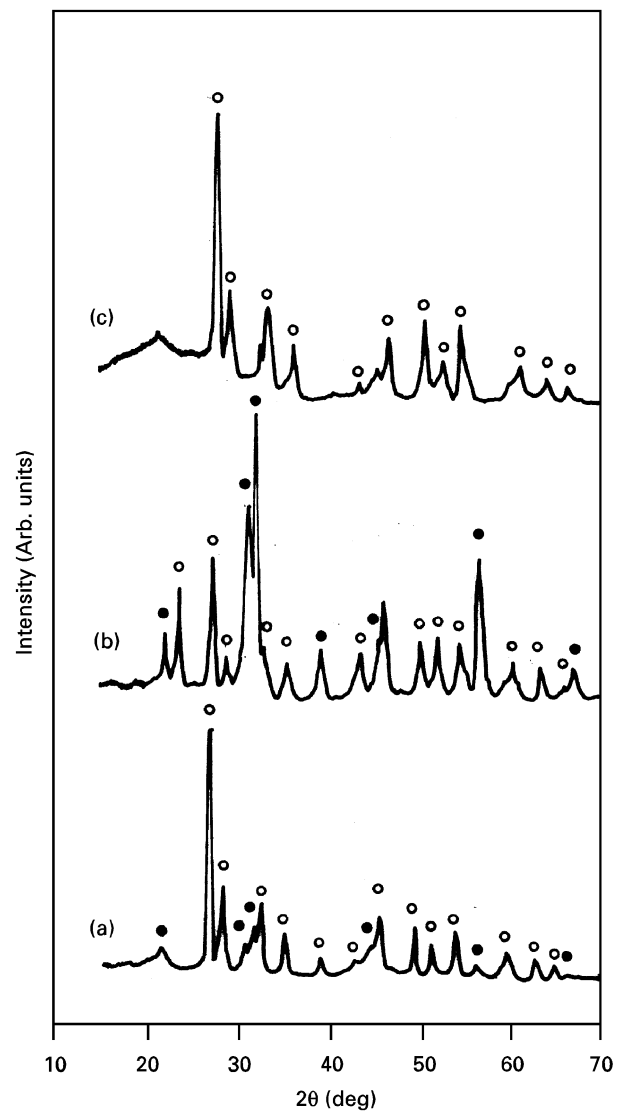


Figure 4 XRD patterns of (a) the ground powder, (b) the bulk surface, and (c) the inner layer of the annealed samples with 200 G magnetic field. (○)  $\gamma$ - $\text{Bi}_2\text{O}_3$ , (●)  $\text{BiFeO}_3$ .

sample shows stronger resonances at  $g = 2.20$  G for the surface layer, as seen in Fig. 5b. The surface layer from the magnetically annealed sample showed an even stronger resonance at  $g = 2.20$  in Fig. 5e. The increase in the resonance intensity at  $g = 2.20$  G, which is ascribed to the octahedral  $\text{Fe}^{3+}$ , could result in the higher volume of  $\text{BiFeO}_3$  crystals at the samples' surface, as seen in the X-ray diffraction patterns.

It has been reported that the oxidation behaviour of the ferrous iron-doped glass is dominated by the chemical diffusion of the divalent cations ( $\text{Fe}^{2+}$ ) from the interior of the glass to the free surface, where they react with the environmental oxygen [24]. However, the effect of the chemical diffusion of  $\text{Fe}^{2+}$  seems to be minor in this study, because the duration of the magnetic annealing process is not long enough for  $\text{Fe}^{2+}$  to migrate a long distance. The oxidation of  $\text{Fe}^{2+}$  would only take place in the vicinity of the sample's surface. The calculated depth of the oxidation layer does not exceed 20 nm. This oxidized state of  $\text{Fe}^{2+}$  with the octahedral coordination would contribute to the formation of  $\text{BiFeO}_3$  ferrite crystals during heat treatment.

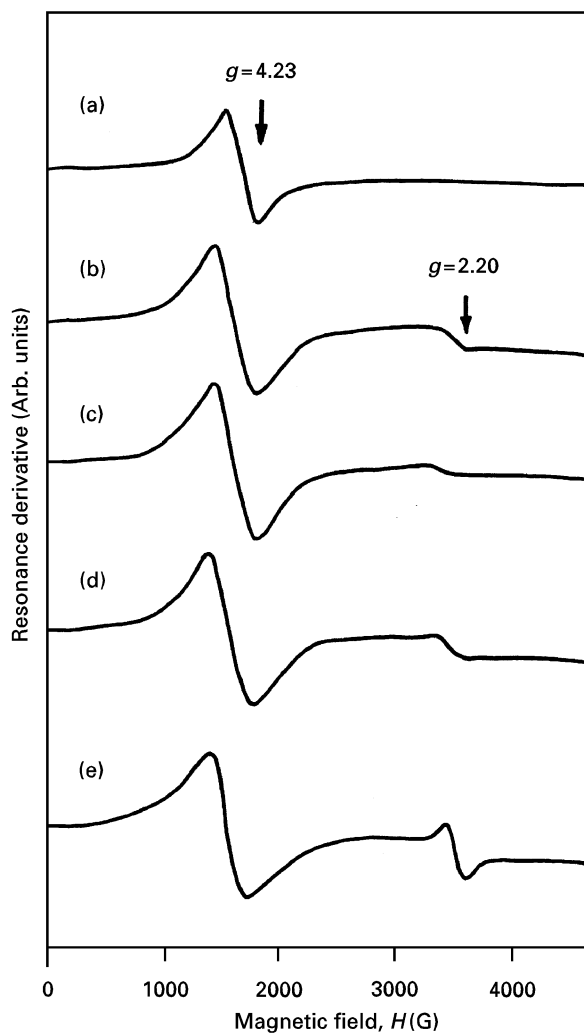


Figure 5 EPR spectra of (a) the original glass, (b) the surface layer of the annealed sample without magnetic field, (c) the annealed sample without magnetic field, (d) the magnetically annealed sample, and (e) the surface layer of the magnetically annealed sample.

TABLE I The EPR results for the glass ceramic samples. The peak intensity is written in relative scale, assuming 100 units to that for the most intense resonance peak observed in the original glass. The thickness of the surface layer for the test was 0.1–0.07  $\mu\text{m}$

| Sample conditions                        | $g$ value (G) | Intensity | $[\text{Fe}^{3+}]_{\text{tet.}} \rightarrow [\text{Fe}^{3+}]_{\text{oct.}}$ % | $[\text{Fe}^{2+}] \rightarrow [\text{Fe}^{3+}]$ oxidation (%) |
|--|---------------|-----------|---|---|
| Original glass                           |               |           |   |   |
| $(g_1)$                                  | 4.23          | 100       | $(100 - g_1)$   | $(g_1 + g_2 - 102)$   |
| $(g_2)$                                  | 2.15          | 2         |   |   |
| Annealed sample (without magnetic field) |               |           |   |   |
| whole sample                             | 4.22          | 98        | 2   | 3   |
|  | 2.20          | 7         |   |   |
| surface layer                            | 4.22          | 96        | 4   | 10  |
|  | 2.21          | 16        |   |   |
| Magnetically annealed sample             |               |           |   |   |
| whole sample                             | 4.23          | 92        | 8   | 4   |
|  | 2.21          | 16        |   |   |
| surface layer                            | 4.22          | 76        | 24  | 11  |
|  | 2.20          | 37        |   |   |

Additionally,  $\text{Fe}^{3+}$  with tetrahedral coordination as exists in the sample could transit to the octahedral state under an applied magnetic field. This can be inferred from the decrease in the intensity of the EPR

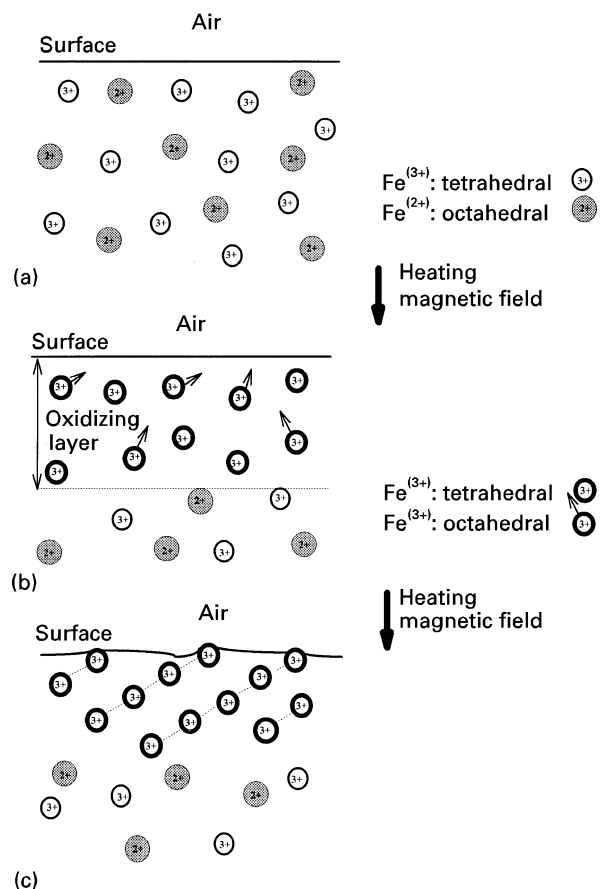


Figure 6 Schematic illustration of the formation mechanism of  $\text{BiFeO}_3$  crystals. (a) Original glass state, random distribution of  $\text{Fe}^{3+}$  and  $\text{Fe}^{2+}$  ions. (b) Oxidation of  $\text{Fe}^{2+}$  and transition and rearrangement of  $\text{Fe}^{3+}$  tet. to  $\text{Fe}^{3+}$  oct. (c) Crystallization and formation of  $\text{BiFeO}_3$  crystals.

resonance at  $g = 4.23$ , as seen in Table I. This transition seems to require excess oxygen and extra space for the rearrangement of  $\text{Fe}^{3+}$  and  $\text{O}^{2-}$ . The surface of the sample provides the proper conditions for the rearrangement. Therefore, the volume of the  $\text{BiFeO}_3$  crystals would largely increase as the volume of  $\text{Fe}^{3+}$  with octahedral coordination increases, as seen in the magnetically annealed samples. The mechanism of the  $\text{BiFeO}_3$  crystalline phase under a magnetic field can be illustrated by two main reactions, as shown in Fig. 6. Oxidation of  $\text{Fe}^{2+}$  and the transition of tetrahedral  $\text{Fe}^{3+}$  to the octahedral coordination takes place before the crystallization of  $\gamma\text{-Bi}_2\text{O}_3$  and  $\text{BiFeO}_3$ . The rearrangement of the  $\text{Fe}^{3+}$  ions would roughen the surface of the magnetic annealed samples. A pattern of eddies has been observed on the surface of the magnetically annealed samples, whereas the samples without magnetic annealing have a smooth surface.

Fig. 7 shows the bulk XRD patterns of the samples under different magnitudes of the applied magnetic field. It was found that the volume fraction of  $\text{BiFeO}_3$  would not significantly increase when the strength of the magnetic field is lower than 150 G. This indicates that the transition of  $\text{Fe}^{3+}$  from 4 to 6 coordination number requires sufficient power to overcome an energy obstacle. Fig. 8a and b are scanning electron micrographs of the etched surfaces of the samples

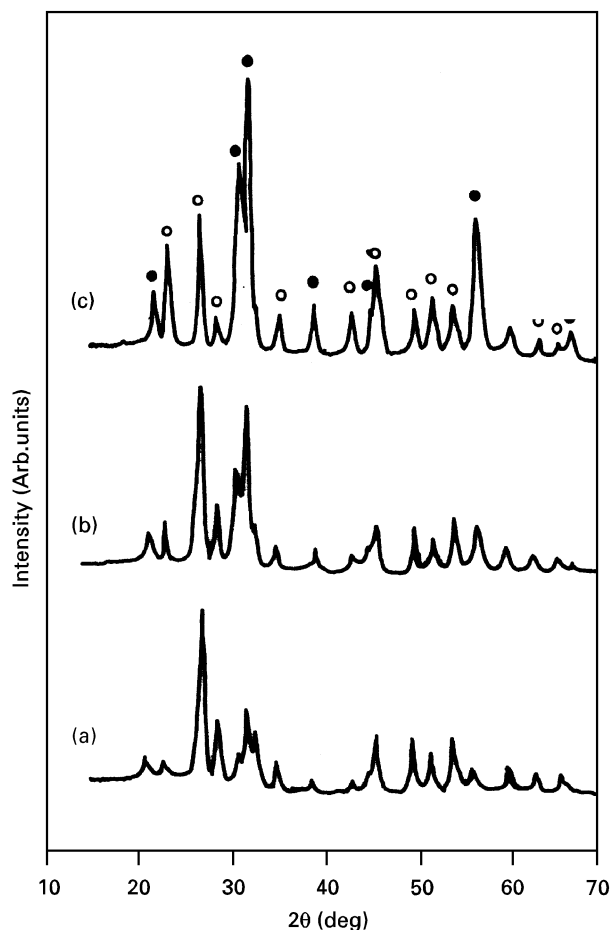


Figure 7 XRD patterns of the glass-ceramic samples with applied magnetic fields of (a) 150 G, (b) 200 G, and (c) 240 G. (○)  $\gamma$ - $\text{Bi}_2\text{O}_3$ , (●)  $\text{BiFeO}_3$ .

without and with magnetic annealing, respectively. It was found that samples with magnetic annealing show finer grains and stronger corrosion resistance.

#### 4. Conclusion

High iron (20%)-containing Bi-Pb-Fe-Cd-O glass was prepared by the melt-quenching process and

a magnetic field was applied during the crystallization process. The crystalline phase after a heat treatment at  $520^\circ\text{C}$  was  $\gamma$ - $\text{Bi}_2\text{O}_3$  with a minor phase of  $\text{BiFeO}_3$ . The formation of crystalline  $\text{BiFeO}_3$  is from the octahedrally coordinated  $\text{Fe}^{3+}$  and is strongly magnetically enhanced at the surface of the samples. Transition of  $\text{Fe}^{3+}$  from tetrahedral to octahedral coordination is encouraged under a magnetic field and, therefore, results in a significant increase in the volume of the  $\text{BiFeO}_3$  phase.

#### Acknowledgement

The author thanks Dr S.-K. Joe for help in setting up the experimental equipment.

#### References

1. R. MULLER, *J. Magn. Magn. Mater.* **101** (1991) 230
2. S. RAM, D. CHAKRAVORTY and D. BAHADUR, *ibid.* **62** (1986) 221.
3. D. BAHADUR, P. K. DAS and D. CHAKRAVORTY, *J. Appl. Phys.* **53** (1982) 7813.
4. J. C. SCLONCZEWSKI, in "Magnetic Materials", Vol. 1, 3rd Edn, edited by F. Brailsford (Wiley, New York, 1960) p. 205.
5. H. PENDER and C. D. GRAHAMN Jr, *Phys. Rev.* **1** (1913) 259.
6. M. GOERTZ, *J. Appl. Phys.* **22** (1951) 964.
7. R. R. SHAW and J. H. HEASLEY, *J. Am. Ceram. Soc.* **50** (1967) 297.
8. B. T. SHIRK and W. R. BUESSEM, *ibid.* **53** (1970) 192.
9. S. RAM, D. BAHADUR and D. CHAKRAVORTY, *J. Magn. Magn. Mater.* **67** (1987) 378.
10. A. BISHAY and C. MAGHRABI, *Phys. Chem. Glasses* **10** (1969) 1.
11. W. H. DUMBAUGH, *ibid.* **19** (1978) 121.
12. *Idem.*, *ibid.* **27** (1986) 119.
13. H. E. KISSINGER, *J. Res. Nat. Bur. Stand.* **57** (1956) 217.
14. B. D. CULLITY (ed.), "Introduction to Magnetic Materials" (Addison-Wesley, London, 1972) p. 35.
15. J. W. MEDERNACH and R. L. SNYDER, *J. Am. Ceram. Soc.* **61** (1978) 494.
16. "X-ray powder diffraction data card file", 11-691, JCPDS 29-235 (American Society for Testing and Materials, Philadelphia, PA, 1978).
17. A. J. JACOBSON and B. E. F. FENDER, *J. Phys. C Solid State Phys.* **8** (1975) 844.

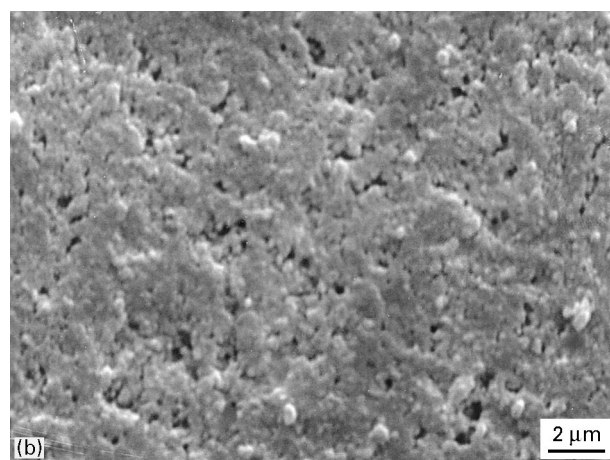
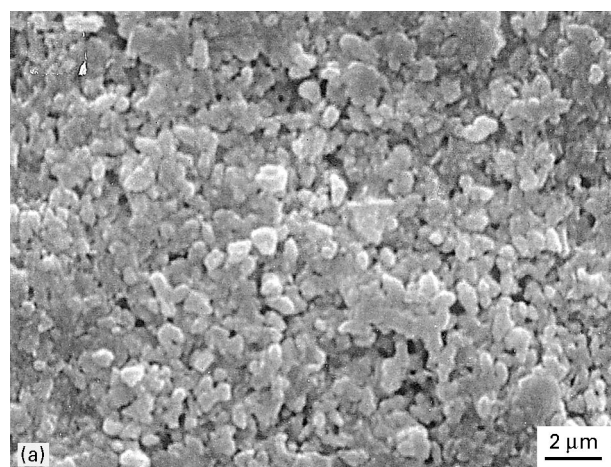


Figure 8 SEM of the etched surface of Bi-Pb-Fe-Cd-O glass-ceramics, (a) without a magnetic field, (b) with 240 G magnetic field.

18. D. LOVERIDGE and S. PARKE, *Phys. Chem. Glasses* **12** (1971) 19.
19. C. HIRAYAMA, J. C. CASTLE and M. KURIYAMA, *ibid.* **9** (1968) 109.
20. M. A. VAYVOD, Y. G. KLYAVA, Z. A. KONSTANS, Y. Y. PURNAS and Y. S. TROKSH, *Fiz. Chim. Stekla (USSR)* **10** (1984) 53.
21. B. O. MYSEN, D. VIRGO, E. R. NEUMANN and F. A. SEIFERT, *Am. Mineral.* **70** (1985) 317.
22. M. P. DICKENSON and P. C. HESS, *Contrib. Mineral. Petrol.* **92** (1986) 207.
23. G. H. BEALL and H. L. RITTLER, *Am. Ceram. Soc. Bull.* **55** (1976) 579.
24. G. B. COOK and R. F. COOPER, *J. Non-Cryst. Solids* **120** (1990) 207.

*Received 9 January  
and accepted 21 May 1996*